



Linking Cr³ triangles through phosphonates and lanthanides: synthetic, structural, magnetic and EPR studies

Journal:	<i>Dalton Transactions</i>
Manuscript ID:	DT-ART-04-2014-001264.R2
Article Type:	Paper
Date Submitted by the Author:	15-Jul-2014
Complete List of Authors:	Zangana, Karzan; University of Manchester, School of Chemistry and Photon Science Institute Pineda, Eufemio; University of Manchester, School of Chemistry and Photon Science Institute Vitorica-Yrzebal, Inigo; University of Manchester, McInnes, Eric; University of Manchester, School of Chemistry Winpenny, R; The University of Manchester, Department of Chemistry

ARTICLE

Linking Cr₃ triangles through phosphonates and lanthanides: synthetic, structural, magnetic and EPR studies

Cite this: DOI: 10.1039/x0xx00000x

Karzan H. Zangana, Eufemio Moreno Pineda, Iñigo J. Vitorica-Yrezabal, Eric J. L. McInnes and Richard E. P. Winpenny*

 Received 00th January 2012,
 Accepted 00th January 2012

DOI: 10.1039/x0xx00000x

www.rsc.org/

The preparation and structural characterisation of five 3d-4f mixed metal phosphonate cages with general formula $[\text{Cr}^{\text{III}}_6\text{Ln}^{\text{III}}_2(\mu_3\text{-O})_2(\text{H}_2\text{O})_2(\text{O}_3\text{P}^t\text{Bu})_4(\text{O}_2\text{C}^t\text{Bu})_{12}(\text{HO}^t\text{Bu})_2(\text{PrNH}_2)_2]$ where $\text{Ln}^{\text{III}} = \text{La}$, **1**; Tb , **3**; Dy , **4**; Ho , **5** and $[\text{Cr}^{\text{III}}_6\text{Gd}^{\text{III}}_2(\mu_3\text{-O})_2(\text{H}_2\text{O})_2(\text{O}_3\text{P}^t\text{Bu})_4(\text{O}_2\text{C}^t\text{Bu})_{12}(\text{HO}^t\text{Bu})_4]$ (**2**) are reported. The structure contains two oxo-centred $\{\text{Cr}_3\}$ triangles, bridged by phosphonates and lanthanides. The magnetic behaviour of **1** has been modelled as two non-interacting isosceles triangles, involving two antiferromagnetic interactions ($J_1 = -8.8 \text{ cm}^{-1}$) with a smaller ferromagnetic interaction for the unique edge of the triangle ($J_2 = +1.3 \text{ cm}^{-1}$) giving an isolated $S = 3/2$ ground state per triangle. The quartet ground state has been proven through simulation of electron paramagnetic resonance (EPR) spectra obtained at X- and Q-band. EPR simulations have also resulted in the introduction of small single-ion Zero Field Splitting (ZFS) parameters $D = \pm 0.19 \text{ cm}^{-1}$ and rhombic term $E = \pm 0.02 \text{ cm}^{-1}$, which are consistent with strong exchange limit calculations for an isolated $S = 3/2$ ($D = \pm 0.22$ and $E = \pm 0.018 \text{ cm}^{-1}$).

Introduction

The synthesis of paramagnetic polymetallic complexes has been an area of significant interest since the discovery of the single molecule magnet (SMM), $[\text{Mn}_{12}\text{O}_{12}(\text{O}_2\text{CMe})_{16}(\text{H}_2\text{O})_4]$.¹ One area of current interest is in making 3d-4f cage compounds, hoping that the combination of strong exchange from the 3d-ions will combine with the large anisotropy of the 4f-ions to produce interesting SMMs. The earliest studies of such 3d-4f heterometallic compounds were by Gatteschi and colleagues, who used designed Schiff-base ligands to bind to both types of metal selectively.² There was also considerable work involving use of anions of 2-hydroxypyridine and its derivatives.³ More recently there has been a huge expansion in this area, with many beautiful new compounds reported.^{4,5}

Phosphonates are multidentate ligands that in their mono or dianionic form can adopt many different coordination modes, with a range of structures and nuclearities containing copper,⁶ iron,⁷ manganese,⁸ nickel,⁹ cobalt^{9c,10} and vanadium.¹¹ More

recently phosphonates have been used for 3d-4f- complexes,^{4n, 5a,c,e,m} and for 4f-compounds.¹²

One of our first forays into this area involved reactions of oxo-centred tri-iron carboxylates with phosphonates,^{7a} where we found that the phosphonate could displace a carboxylate and link triangles together. Frequently we found that additional reactions occurred, with an iron centre extracted from a triangle to bind to the phosphonate separately. This produced compounds containing four (one triangle plus one iron) and seven (two triangles bridged by one iron) metals.^{7a} We reasoned that if we used more stable oxo-centred triangles, and deliberately added a source of a second metal we could make similar arrays, but heterometallic. Therefore we have undertaken the reaction of oxo-centred chromium(III) carboxylates with phosphonates in the presence of lanthanide ions.

In this paper we report the synthesis, structural characterisation, and magnetic properties of a series of octanuclear $\text{Cr}^{\text{III}}\text{-Ln}^{\text{III}}$ phosphonate cages ($\text{Ln}^{\text{III}} = \text{La}$, **1**; Gd , **2**; Tb , **3**; Dy , **4**; Ho , **5**) using ^tbutyl phosphonic acid as ligand. We were able to single out the contribution of Ln^{III} by comparing **2**, **3**, **4** and **5** with the lanthanum analogue **1**; this family of cages provides a good opportunity to systematically study the magnetic exchange between 3d and 4f metal ions.

School of Chemistry and Photon Science Institute, The University of Manchester, Oxford Road, Manchester M13 9PL, UK. Fax: 44-161-275-1001; E-mail: richard.winpenny@manchester.ac.uk

† Electronic Supplementary Information (ESI) available: further crystallographic details.

See DOI: 10.1039/b000000x/

‡ Deposit number CCDC 999505 – 999509

Experimental Section

Material and physical measurements

$[\text{Cr}^{\text{III}}_3(\mu_3\text{-O})(\text{O}_2\text{C}^t\text{Bu})_6(\text{H}_2\text{O})_3][\text{O}_2\text{C}^t\text{Bu}] \cdot 3\text{H}_2\text{O}$ was synthesised according to reported methods.¹³ All reagents, metal salts, solvents and ligands were used as purchased without any further purification. Analytical data were obtained by the microanalytical service of the University of Manchester. The data and yields are given in Table 1.

Table 1. Elemental analysis and yield (%) for compounds 1–5

Cage	Yield ^a	Elemental analysis: Found (calculated)					
		C	H	Cr	Ln	P	N
1-b	40%	41.33	7.32	10.58	9.41	4.19	0.94
		(41.06)	(7.38)	(10.88)	(9.69)	(4.32)	(0.98)
2-b	31%	41.15	7.16	10.97	10.80	4.33	-
		(40.95)	(7.28)	(10.64)	(10.72)	(4.21)	(-)
3-c	30%	41.09	7.38	10.48	11.21	4.10	0.93
		(40.75)	(7.26)	(10.80)	(11.00)	(4.27)	(0.97)
4-c	29%	40.48	7.43	10.42	11.35	4.11	0.90
		(40.65)	(7.24)	(10.77)	(11.22)	(4.28)	(0.97)
5-d	22%	40.89	6.79	10.53	10.97	4.07	0.93
		(40.84)	(7.20)	(10.82)	(11.44)	(4.30)	(0.97)

a. Based on phosphonate source. Calculated EA and crystallisation solvents: b = 2(HO^tBu)·2(H₂O); c = 2(HO^tBu)·(H₂O) and d = 2(HO^tBu).

Synthesis

$[\text{Cr}^{\text{III}}_3(\mu_3\text{-O})(\text{O}_2\text{C}^t\text{Bu})_6(\text{H}_2\text{O})_3][\text{O}_2\text{C}^t\text{Bu}]$ (1 g, 1.225 mmol), Gd(NO₃)₃·6H₂O (0.554 mmol), *t*-butyl phosphonic acid (0.07 g, 0.507 mmol) and isopropylamine (ⁱPrNH₂) (0.1 mL, 1.164 mmol) in isobutanol (HO^tBu)(15 mL) were refluxed at 120 °C for 24 hours to form a dark green solution. The solution was filtered and then allowed to stand undisturbed at room temperature. Green plate-like crystals suitable for single crystal X-ray diffraction of $[\text{Cr}^{\text{III}}_6\text{Gd}^{\text{III}}(\mu_3\text{-O})_2(\text{H}_2\text{O})_2(\text{O}_3\text{P}^t\text{Bu})_4(\text{O}_2\text{C}^t\text{Bu})_{12}(\text{HO}^t\text{Bu})_4]$ (**2**) were collected after 10 days. Similar reactions with Ln^{III}(NO₃)₃·*n*H₂O, where Ln^{III} = La(**1**), Tb(**3**), Dy(**4**) and Ho(**5**) gave crystals of $[\text{Cr}^{\text{III}}_6\text{Ln}^{\text{III}}_2(\mu_3\text{-O})_2(\text{H}_2\text{O})_2(\text{O}_3\text{P}^t\text{Bu})_4(\text{O}_2\text{C}^t\text{Bu})_{12}(\text{HO}^t\text{Bu})_2(^i\text{PrNH}_2)_2]$ (Table 1).

X-ray data collection and structure solution

Data collection was carried out on Agilent SUPERNOVA diffractometer with MoK α radiation ($\lambda = 0.71073 \text{ \AA}$), data reduction and unit cell refinement were performed with CrysAlisPro software. The structures were solved by direct method using SHELXS-97^{14a} and were refined by full-matrix least-squares calculations on F^2 using the program Olex2.^{14b} Suitable crystals of **1–5** were mounted on a tip using crystallographic oil and placed in a cryostream and used for data collection. Data were collected using ϕ and ω scans chosen to give a complete asymmetric unit. All non-hydrogen atoms were refined anisotropically. Hydrogen atoms were calculated geometrically and were riding on their respective atoms. Hydrogens corresponding to disorder water molecules and hydroxyl groups form solvated isobutanol molecules were omitted but included in the formula. Some degree of disorder was found in all cages. The ^tBu groups of the pivalates, ^tBu groups of the phosphonates, the coordinated and uncoordinated (only compound **2**) isobutanol and isopropylamine are found to be disordered over two sites. These disordered groups were modelled splitting their occupancy into two parts. The isobutanol solvent molecules were found to be disordered over three sites for compound **1,3-5**. These disordered molecules were modelled splitting their occupancy into three parts and restraining their value to add 1 using the SUMP command. The amount of uncoordinated solvent was determined using SQUEEZE. The number of electrons calculated agrees with two isobutanol and two water molecules per unit cell for compounds **1,3-5**. For compound **2**, it was found to have four isobutanol and eight water molecules per unit cell. The C-C distances of the ^tBu groups of the pivalates and the phosphonates were restrained to be equal using SADI command. The C-C, C-O and C-N distances for both the isopropylamine and the isobutanol were restrained using DFIX command. The atomic displacement parameters of the disorder moieties were restrained using RIGU command. Full crystallographic details can be found in CIF format: CCDC for **1-5**, 999505–999509. Crystal data and refinement parameters are given in Table 2.

Table 2. Crystallographic information for Cages 1–5.

	1 · 2^tBuOH · 2H₂O	2 · 2^tBuOH · 4H₂O	3 · 2^tBuOH · 2H₂O	4 · 2^tBuOH · 2H₂O	5 · 2^tBuOH · 2H₂O
chem formula	C ₉₈ H ₂₁₀ Cr ₆ La ₂ N ₂ O ₄₆ P ₄	C ₁₀₀ H ₂₁₀ Cr ₆ Gd ₂ O ₅₀ P ₄	C ₉₈ H ₂₁₀ Cr ₆ N ₂ O ₄₆ P ₄ Tb ₂	C ₉₈ H ₂₁₀ Cr ₆ Dy ₂ N ₂ O ₄₆ P ₄	C ₉₈ H ₂₁₀ Cr ₆ Ho ₂ N ₂ O ₄₆ P ₄
fw	2866.37	2957.00	2906.39	2913.55	2916.83
cryst system	triclinic	monoclinic	triclinic	triclinic	triclinic
space group	<i>P</i> -1	<i>P</i> ₂ / <i>n</i>	<i>P</i> -1	<i>P</i> -1	<i>P</i> -1
<i>a</i> /Å	13.7609(5)	13.8020(7)	13.918(1)	13.7094(6)	13.7501(4)
<i>b</i> /Å	13.9671(5)	27.527(2)	14.0369(7)	14.0352(5)	14.0220(5)
<i>c</i> /Å	23.3521(8)	19.718(2)	23.346(2)	23.1626(9)	23.1827(8)
α /°	100.081(3)	90	99.776(5)	100.096(3)	100.079(3)
β /°	100.916(3)	95.817(7)	101.128(6)	100.639(3)	100.637(3)
γ /°	107.940(3)	90	108.202(5)	108.186(4)	108.254(3)
<i>V</i> /Å ³	4059.8(3)	7453(1)	4119.7(5)	4029.8(3)	4040.0(2)
<i>Z</i>	1	2	1	1	1
ρ calcd/g cm ⁻³	1.172	1.295	1.171	1.201	1.199
<i>T</i> /K	150(1)	150.0(2)	210.1(2)	150.0(1)	150.0(1)
μ (Mo K α)/mm ⁻¹	1.003	1.412	1.328	1.407	1.458
R_1 ($I > 2\sigma(I)$) ^a	0.0753	0.0777	0.0664	0.0661	0.0637
wR_2 ^a (all data)	0.2342	0.2048	0.2045	0.2052	0.2055

^a $R_1 = \frac{\sum ||F_o| - |F_c||}{\sum |F_o|}$, $wR_2 = \left[\frac{\sum w(|F_o| - |F_c|)^2}{\sum w|F_o|^2} \right]^{1/2}$

Magnetic measurements

The magnetic properties of polycrystalline samples of **1** – **5** were measured in the temperature range 1.8 K – 300 K with a Quantum Design MPMS-XL7 SQUID magnetometer armed with a 7 T magnet. The samples were ground, placed in a gel capsule, and fixed with a small amount of eicosane to avoid movement during the measurement. The data were corrected for the diamagnetism from the gel capsule and the eicosane with the diamagnetic contribution from the complexes calculated from Pascal constants. Magnetic data were fitted using the program PHI.¹⁵

Electron Paramagnetic Resonance

X-band (*ca.* 9.5 GHz) and Q-band (*ca.* 34 GHz) EPR spectra of polycrystalline powders were recorded with a Bruker EMX580 spectrometer. The data was collected in the temperature range 5 – 30 K using liquid helium. Spectral simulations were performed using the *EasySpin* 4.5.5¹⁶ simulation software.

Result and discussion

Synthetic description

Many synthetic procedures rely on the reaction of oxo-centred metal triangles,^{7,8,17} however fewer reactions use chromium oxo-centred triangles $[\text{Cr}^{\text{III}}_3(\mu_3\text{-O})(\text{RCO}_2)_6(\text{L})_3]\text{X}$ (R = Me, Ph, ^tBu; X = Cl, NO₃) and in many of those reactions the triangle is not found in the final product.¹⁸ However here we find that refluxing a mixture of chromium pivalate oxo-centred triangle $[\text{Cr}^{\text{III}}_3(\mu_3\text{-O})(\text{O}_2\text{C}^t\text{Bu})_6(\text{H}_2\text{O})_3][\text{O}_2\text{C}^t\text{Bu}] \cdot 3\text{H}_2\text{O}$, hydrated lanthanide nitrate, $\text{Ln}^{\text{III}}(\text{NO}_3)_3 \cdot n\text{H}_2\text{O}$, phosphonic acid, $\text{H}_2\text{O}_3\text{P}^t\text{Bu}$, and a mild base, ^tPrNH₂, in ^tBuOH in the mole ratios 1.2 : 0.50 : 0.50 : 1.2 gives reasonable yields of a family of $\{\text{Cr}_6\text{Ln}_2\}$ cages Ln = La **1**, Gd **2**, Tb **3**, Dy **4** and Ho **5**.

Crystallography

The cages **1-5** crystallise in two different space groups monoclinic $P2_1/n$ (**2**) and triclinic $P-1$ (**1**, **3**, **4** and **5**) (Figure 1), however the molecular structures are very similar and we describe the structure of **1** as representative. Overall the structure contains six Cr^{III} and two La^{III} ions, which are held together by two μ_3 -oxide and four phosphonates beside ten bridging pivalates. The octanuclear cage consists of two equivalent oxo-centered chromium triangles $\{\text{Cr}^{\text{III}}_3(\mu_3\text{-O})\}$.

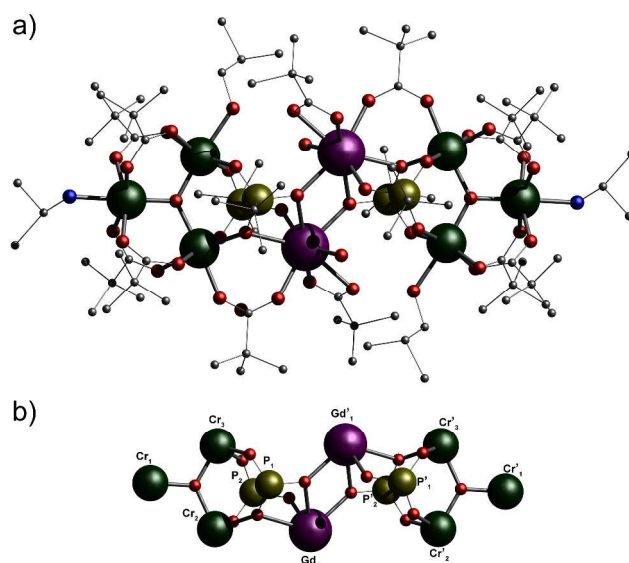


Figure 1. Crystal structure of the $\{\text{Cr}_6\text{Gd}_2\text{P}_4\}$ cage **1**. a) Top left: top view of cage. b) Metal core of cage **1** without carbons. Scheme: La, purple; Cr, dark green; P, light green; O, red; C, grey; N, cyan; H omitted for clarity.

In each triangle two edges are bridged by 2.11 pivalates (Harris notation)¹⁹ (Supporting Information, Figure S1), as in the starting material, but on the third edge both pivalates have been displaced by phosphonates. These phosphonates bridge the Cr...Cr edge, but use their third oxygen atom to bind to a La^{III} site; in one phosphonate (and its symmetry equivalent) the oxygen bridges between two La^{III} sites, given it a 4.211 binding mode. In the other pair of symmetry equivalent phosphonates the third O-atom is terminal to a La^{III}, giving it the 3.111 binding mode. A 2.11 bridging pivalate also bridges between on Cr site, occupying the position *trans* to the μ_3 -oxide, and a lanthanum. This site is occupied by a terminal ^tBuOH for the other four Cr sites (Figure 1).

The distance between the two μ_3 -oxides and the three Cr^{III} ions within triangles fall in the range 1.8924(1) – 1.94955(8) Å, the Cr–O–Cr angles are very close to 120° and sum to 360° (Supporting Information, Table S1 and Figure S4).

The Cr–Cr distances within the triangles fall in the range 3.2351(2) – 3.4275(5) Å, while the La–La' distance within the cage is 4.192(8) Å. In **2**, all Cr^{III} centres have an O₆ coordination sphere, with octahedral coordination geometry; whilst in the remaining analogues a terminal amine fill the coordination sphere of Cr1 and Cr(1)', leading to a O₅N set, and a O₆ coordination sphere for Cr(2), Cr(3), Cr(2)' and Cr(3)'. The Ln^{III} ion centres have an LnO₈ coordination sphere, consisting of four oxygen atoms from the phosphonate bridging groups, three oxygens belonging to two pivalates and one water oxygen atom (Supporting Information, Figures S2 and S3).

Magnetic description

We have studied the magnetic behaviour of complexes **1-5** using polycrystalline samples in the temperature range 2 – 300 K under 1000 Oe applied magnetic field. Similarly we have investigated the magnetisation as function of applied magnetic

field (H) at 2 and 4 K in the range of 0 – 7 T. The temperature dependence of the $\chi_M T(T)$ (where χ_M is the molar magnetic susceptibility) for all polycrystalline samples show values lower than expected for the single ion contribution of six Cr^{III} $S = 3/2$ and the paramagnetic lanthanide contribution e.g. the contribution from Gd^{III} , Tb^{III} , Dy^{III} or Ho^{III} for **2** – **5** respectively. Complex **1** shows a $\chi_M T$ at room temperature of $9.6 \text{ cm}^3 \text{ K mol}^{-1}$ considerably lower than expected (calcd. $11.1 \text{ cm}^3 \text{ K mol}^{-1}$ for six Cr^{III} : $g_{\text{Cr}} = 1.99$, $S = 3/2$). For complex **1** $\chi_M T(T)$ decreases with lowering temperature reaching a value of $3.6 \text{ cm}^3 \text{ K mol}^{-1}$ at 2 K suggesting, along with the $\chi_M T(T)$ value at room temperature, antiferromagnetic interactions between the Cr sites in the cage. Complexes **2** to **5** exhibit similar

behaviour: for **2** the $\chi_M T$ room temperature value is $23.3 \text{ cm}^3 \text{ K mol}^{-1}$ (calcd. $26.7 \text{ cm}^3 \text{ K mol}^{-1}$ for six Cr^{III} : $g_{\text{Cr}} = 1.99$, $S = 3/2$ and two Gd^{III} : $g_{\text{Gd}} = 1.99$; $S = 7/2$) which gradually decreases to 20 K where it sharply decreases to $15.9 \text{ cm}^3 \text{ K mol}^{-1}$ at 2 K indicating that at this temperature paramagnetic states are still populated; **3** to **5** reveal room temperature $\chi_M T$ values of $33.2 \text{ cm}^3 \text{ K mol}^{-1}$ (calcd. $34.8 \text{ cm}^3 \text{ K mol}^{-1}$ for six Cr^{III} : $g_{\text{Cr}} = 1.99$, $S = 3/2$ and two Tb^{III} : $g_{\text{Tb}} = 3/2$; $J = 6$), $38.1 \text{ cm}^3 \text{ K mol}^{-1}$ (calcd. $39.5 \text{ cm}^3 \text{ K mol}^{-1}$ for six Cr^{III} : $g_{\text{Cr}} = 1.99$, $S = 3/2$ and two Dy^{III} : $g_{\text{Dy}} = 4/3$; $J = 15/2$) and $37.6 \text{ cm}^3 \text{ K mol}^{-1}$ (calcd. $39.3 \text{ cm}^3 \text{ K mol}^{-1}$ for six Cr^{III} : $g_{\text{Cr}} = 1.99$, $S = 3/2$ and two Ho^{III} : $g_{\text{Ho}} = 5/4$; $J = 8$) mol^{-1} respectively (Figure 2).

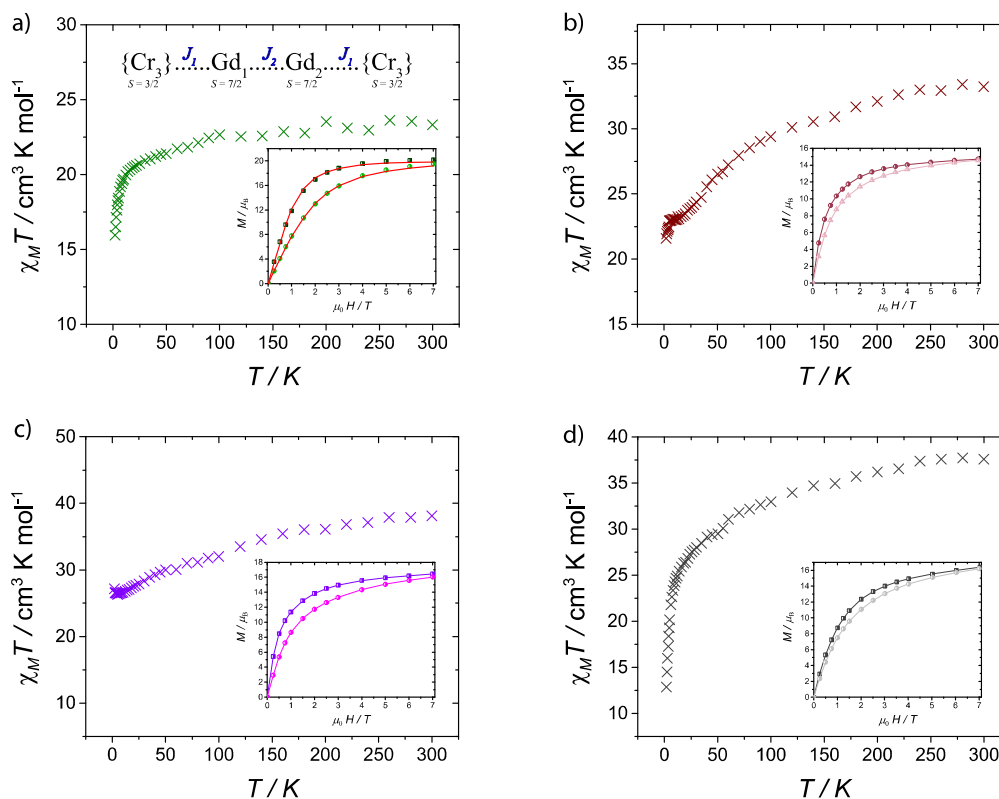


Figure 2. (Left) Molar magnetic susceptibility ($\chi_M T$) vs. T plot for **2** - **5** under 1 kG dc field and molar magnetization (M) as a function of applied magnetic field (H) at 2 and 4 K (inset) for a) **2**, b) **3**, c) **4** and d) **5**.

The temperature dependent susceptibility gradually decreases upon lowering temperature for all complexes, however at low temperature two different behaviours are observed. For complex **3** a small plateau is observed from ca. 13 to 5 K, before dropping to $21.6 \text{ cm}^3 \text{ K mol}^{-1}$ at 2 K . In the case of complex **4** the gradual decrease in $\chi_M T(T)$ upon lowering temperature stops at about 8 K where it starts gradually to increase up to $27.2 \text{ cm}^3 \text{ K mol}^{-1}$ at 2 K . The behaviour exhibited by **3** and **4** suggest some ferromagnetic interactions, probably between the 3d-4f system.¹⁻⁴ Complex **5** decreases gradually up to ca. 40 K where it drops sharply to $12.9 \text{ cm}^3 \text{ K mol}^{-1}$ indicating antiferromagnetic interactions and/or depopulation of the Stark sublevels (see Figure 2).

The molar magnetisation (M) as function of applied magnetic field at 2 K in the field range of 0 – 7 T shows a saturation value at 7 T for compounds **1** and **2** of 5.9 and $20.2 \mu_{\text{B}}$. Complex **3** to **5** show $M(H)$ values of 14.7 for the **3** and $16.4 \mu_{\text{B}}$ for the other two. No conclusion can be drawn from the field dependence for **3** to **5** due to the high anisotropy presented for these lanthanide-containing cages.

The magnetic behaviour of **1** was modelled using PHI package,¹⁵ fitting $\chi_M T(T)$ and $M(H)$ simultaneously. As **1** contains La^{III} , study of this compound allows the determination of the exchange interaction within the two $\{\text{Cr}_3\}$ moieties. A simple model has been used based on the sum of two non-interacting $\{\text{Cr}_3\}$ triangles (based on the crystallographic data,

the nearest Cr₃...Cr₃ distance from each triangle is 9.289(1) Å. Each {Cr₃} triangle has been modelled using a Hamiltonian of the form (1):

$$H = -2J_1(\hat{S}_1\hat{S}_2 + \hat{S}_1\hat{S}_3) - 2J_2(\hat{S}_2\hat{S}_3) + g\mu_B H \sum_{i=1}^3 \hat{S}_i \quad (1)$$

where the first term is the isotropic exchange interaction between Cr(1)...Cr(2) and Cr(2)...Cr(3), and the second term that between Cr(1)...Cr(3), the chemically unique edge (Figure 3). The fourth term is the Zeeman term of each Cr centre.

Good agreement between experiment and simulation for $\chi_M T$ vs. T and M vs. H is also obtained including a small ZFS (see below). Simultaneous fitting of $\chi_M T(T)$ and $M(H)$ yield agreement between experimental data and simulation with an antiferromagnetic exchange interaction $J_1 = -8.8 \text{ cm}^{-1}$, and a ferromagnetic interaction of $J_2 = +1.3 \text{ cm}^{-1}$ between the Cr ions in the unique edge of the triangle, giving a total spin ground state for each individual {Cr₃} fragment of $S = 3/2$ (see figure 3), with the first excited state, $S = 1/2$, at 33 cm^{-1} above it. The field dependence of the magnetisation can be reproduced using the Brillouin function for two $S = 3/2$ states, which suggests there is very little communication between the two {Cr₃} triangles in the {Cr₆La₂} cage (Figure 4).

Attempts to investigate the magnetic behaviour of **2** were made, however due to the huge Hilbert space $((2S_i + 1)^n \times (2S_j + 1)^n = 262144)$ for the six Cr^{III} ($S = 3/2$) and two Gd^{III} ($S = 7/2$), the system is rendered quite difficult for the evaluation of its Hamiltonian. To overcome this issue the magnetic data of **2** was modelled assuming two {Cr₃} with $S = 3/2$, obtained from the magnetic behaviour of **1** and the EPR data (see below) and two Gd^{III}. We have used a simple Hamiltonian (2) considering a linear combination of Cr...Gd...Gd...Cr (see inset Figure 2a).

$$H = -2J_1(\hat{S}_1\hat{S}_2 + \hat{S}_3\hat{S}_4) - 2J_2(\hat{S}_2\hat{S}_3) + g\mu_B H \sum_{i=1}^4 \hat{S}_i \quad (2)$$

Simultaneous fitting of $M(H)$ at 2 and 4 K resulted in ferromagnetic interactions between each {Cr₃} and the neighbour Gd^{III} $J_1 = +0.19 \text{ cm}^{-1}$, whilst a small antiferromagnetic interaction was obtained for the Gd...Gd pair $J_2 = -0.08 \text{ cm}^{-1}$.

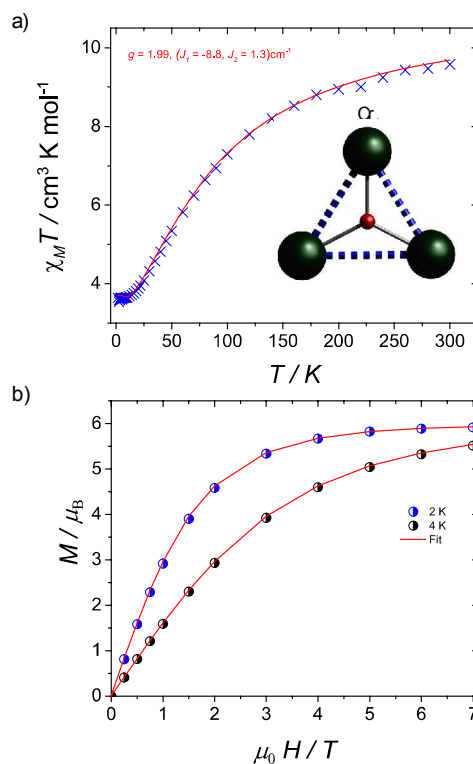


Figure 3. (Left) Molar magnetic susceptibility ($\chi_M T$) vs. T and simulation plots for **1** under 1 kG dc field. Right: Molar magnetization (M) as a function of applied magnetic field (H) at 2 and 4 K for **1**.

Electron paramagnetic resonance

EPR spectroscopy has generally been an important tool in probing the spin ground states of molecular complexes.²⁰ The EPR spectroscopy of **1** was studied in the temperature range of 5 – 30 K using X- and Q-band frequencies, *ca.* 9.5 GHz and 34.5 GHz respectively. Several features are observed in X-band EPR at 5 K (Figure 5). Broad intense transitions are observed at 60, 160 and 440 mT resonance fields, whilst a less intense signal is observed at about 350 mT ($g \sim 2$). Upon raising the temperature the intense signals decrease while the minor signal at $g \sim 2$ sharply increases, suggesting the population of an excited state, probably $S = 1/2$ (see below). The Q-band EPR data shows similar behaviour, with several features at 5 K, which broaden upon raising the temperature, whilst the signal at $g \sim 2$ sharply increases.

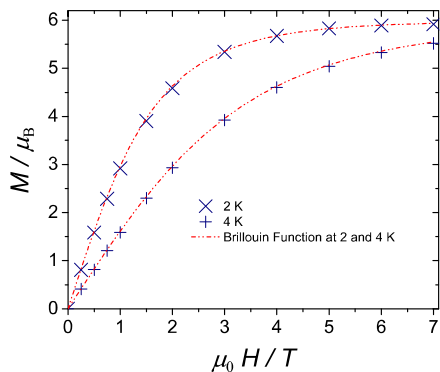


Figure 4. Magnetisation of complex **1** and Brillouin function (red line) for two $S = 3/2$ states at 2 and 4 K.

We have simulated the X- and Q-band EPR data using the parameters obtained from fitting the magnetic data (see above), with inclusion of axial (D) and rhombic (E) ZFS terms, giving Hamiltonian (3):

$$H = -2J_1(\hat{S}_1\hat{S}_2 + \hat{S}_2\hat{S}_3) - 2J_2(\hat{S}_1\hat{S}_3) + D\sum_{i=1}^3 S_{iz}^2 + E\sum_{i=1}^3(S_{ix}^2 - S_{iy}^2) + g\mu_B H\sum_{i=1}^3 \hat{S}_i \quad (3)$$

Agreement between experimental data was achieved using the parameters above with $D_{Cr} = \pm 0.19 \text{ cm}^{-1}$ and $E_{Cr} = \pm 0.02 \text{ cm}^{-1}$ (Figure 5a and b). Inclusion of these small ZFS terms in the fit of magnetic data makes little difference to the quality of the fit.

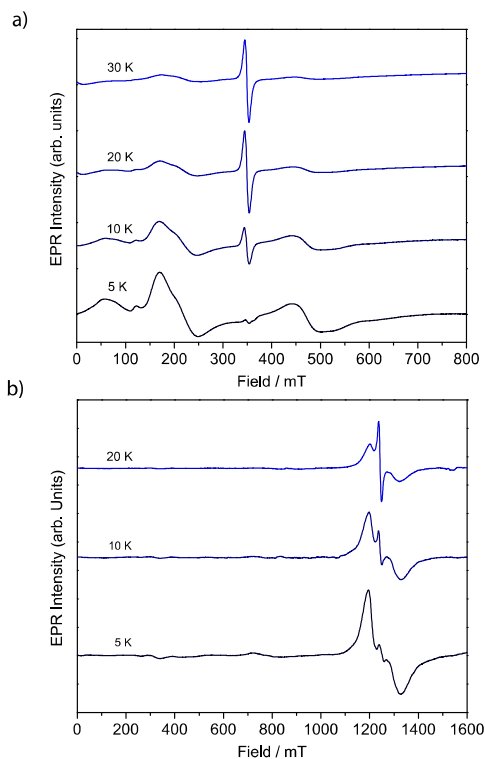


Figure 5. (a) X-band spectrum for compound **1** in the temperature range of 5 – 30 K; (b) Q-band spectrum for compound **1** in the temperature range of 5 – 20 K.

The EPR behaviour can also be modelled in the strong exchange limit as an isolated $S = 3/2$ state with $D_{3/2} = \pm 0.22 \text{ cm}^{-1}$ and $E_{3/2} = \pm 0.018 \text{ cm}^{-1}$ revealing an isolated quartet state with nearly no contribution from excited states present at 5 K (see figure 5c and d). If the strong exchange limit is valid here, the vector coupling method of Bencini and Gatteschi²¹ would give $D_{3/2} = 29D_{Cr}/25$. Our two values for the zero-field splitting are entirely consistent with one another, demonstrating that use of the strong exchange limit is reasonable.

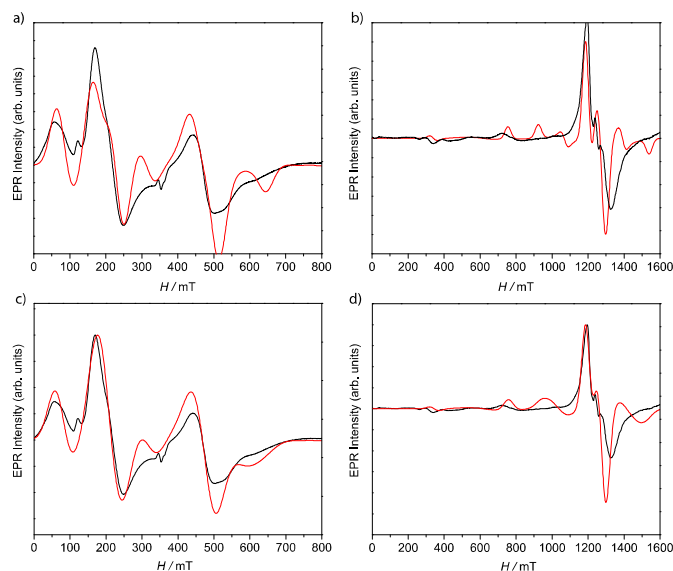


Figure 5. (a) X-band and (b) Q-band spectra (black trace) and simulation (red trace) for compound **1** modelled as exchange coupled system at 5 K ($S = 3/2$; $g_{Cr} = 1.99$; $D = \pm 0.19$; $E = \pm 0.02$, $J_1 = +1.8$, $J_2 = -8.8 \text{ cm}^{-1}$); (c) X-band and (d) Q-band spectra (black trace) and simulation (red trace) for compound **1** at 5 K modelled as $S = 3/2$ $g_{Cr} = 1.99$; $D = \pm 0.22$; $E = \pm 0.018 \text{ cm}^{-1}$.

Conclusions

To summarise, by using an oxo-centered chromium pivalate triangles complex as a starting material reacted with a range of different lanthanide starting materials and using *t*-butylphosphonate as a ligand we have obtained a range of 3d-4f mixed metal octanuclear complexes. The precursor $\{\text{Cr}_3\}$ triangles can be recognized in all the resulting cages, and there is a relation to the $\{\text{Fe}_7\}$ cages we have reported previously,^{7a} where a single Fe^{III} ion bound to the phosphonates, linking triangles. At present we cannot control or predict how the phosphonates assemble the 4f-ions in order to form larger cages, but it appears this is a valuable strategy for synthesizing moderately large polymetallic cages.

Acknowledgements

KZ thanks the KRG-Scholarship program in ‘‘Human Capacity Development (HCDP)’’. E.M.P. thanks the Panamanian agency SENACYT-IFARHU. REPW thanks the Royal Society for a Wolfson Merit Award. We thank the EPSRC(UK) for funding for an X-ray diffractometer (grant number EP/K039547/1).

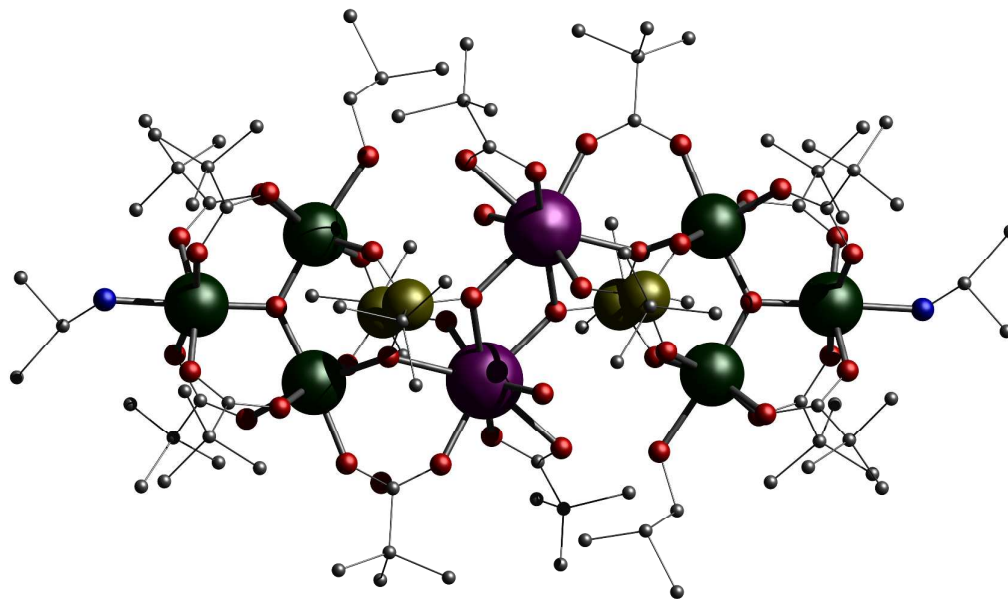
References

1. R. Sessoli, D. Gatteschi, A. Caneschi and M. A. Novak, *Nature*, 1993, **365**, 141; (b) R. Sessoli, H. L. Tsai, A. R. Schake, S. Y. Wang, J. B. Vincent, K. Folting, D. Gatteschi, G. Christou and D. N. Hendrickson, *J. Am. Chem. Soc.*, 1993, **115**, 1804.
2. (a) A. Bencini, C. Benelli, A. Caneschi, R. L. Carlin, A. Dei, and D. Gatteschi, *J. Am. Chem. Soc.*, 1985, **107**, 8128; (b) A. Bencini, C. Benelli, A. Caneschi, A. Dei and Gatteschi, *D. Inorg. Chem.* 1986, **25**, 572; (c) C. Benelli, A. Caneschi, D. Gatteschi, O. Guillou and L. Pardi *Inorg. Chem.* 1990, **29**, 1750.
3. R. E. P. Winpenny, *Chem. Soc. Rev.*, 1998, **27**, 447 and refs therein.
4. (a) A. Mishra, A.J. Tasiopoulos, W. Wernsdorfer, E.E. Moushi, B. Moulton, M.J. Zaworotko, K.A. Abboud, G Christou, *Inorg. Chem.*, 2008, **47**, 4832; (b) R. Sessoli and A. K. Powell, *Coord. Chem. Rev.*, 2009, **253**, 2241; (c) S. K. Langley, L. Ungur, N. F. Chilton, B. Moubaraki, L. F. Chibotaru and K. S. Murray, *Chem. Eur. J.*, 2011, **17**, 9209; (d) T. D. Pasatoiu, M. Etienne, A. M. Madalan, M. Andruh and R. Sessoli, *Dalton Trans.*, 2010, **39**, 4802; (e) C. G. Efthymiou, T. C. Stamatatos, C. Papatriantafyllopoulou, A. J. Tasiopoulos, W. Wernsdorfer, S. P. Perlepes and G. Christou, *Inorg. Chem.*, 2010, **49**, 9737; (f) G. Rigaux, R. Inglis, S. Morrison, A. Prescimone, C. Cadiou, M. Evangelisti and E. K. Brechin, *Dalton Trans.*, 2011, **40**, 4797; (g) Y. Gao, L. Zhao, X. Xu, G.-F. Xu, Y.-N. Guo, J. Tang and Z. Liu, *Inorg. Chem.*, 2011, **50**, 1304; (h) C. Papatriantafyllopoulou, W. Wernsdorfer, K. A. Abboud and G. Christou, *Inorg. Chem.*, 2011, **50**, 421; (i) A. Saha, M. Thompson, W. Wernsdorfer, K. A. Abboud and G. Christou, *Inorg. Chem.*, 2011, **50**, 10476; (j) Y.-F. Zeng, G.-C. Xu, X. Hu, Z. Chen, X.-H. Bu, S. Gao and E. C. Sañudo, *Inorg. Chem.*, 2010, **49**, 9734; (k) H. L. C. Feltham, R. Clérac, A. K. Powell and S. Brooker, *Inorg. Chem.*, 2011, **50**, 4232; (l) E. Colacio, J. Ruiz-Sanchez, F. J. White and E. K. Brechin, *Inorg. Chem.*, 2011, **50**, 7268; (m) M. Hołyńska, D. Premužić, I.-R. Jeon, W. Wernsdorfer, R. Clérac and S. Dehnen, *Chem. Eur. J.*, 2011, **17**, 9605; (n) V. Baskar, K. Gopal, M. Helliwell, F. Tuna, W. Wernsdorfer and R.E.P. Winpenny, *Dalton Trans.*, 2010, **39**, 4747.
5. (a) Y.-Z. Zheng, M. Evangelisti, R. E. P. Winpenny, *Angew. Chem., Int. Ed.* 2011, **50**, 3692; (b) R. Sessoli and A. K. Powell, *Coord. Chem. Rev.*, 2009, **253**, 2241; (c) Y.-Z. Zheng, E. M. Pineda, M. Helliwell, M. Evangelisti, R. E. P. Winpenny, *Chem. Eur. J.*, 2012, **18**, 4161; (d) M. Wang, D.-Q. Yuan, C.-B. Ma, M.-J. Yuan, M.-Q. Hu, N. Li, H. Chen, C.-N. Chen and Q.-T. Liua, *Dalton Trans.*, 2010, **39**, 7276; (e) Y.-Z. Zheng, M. Evangelisti, F. Tuna and R. E. P. Winpenny, *J. Am. Chem. Soc.* 2012, **134**, 1057; (f) T. N. Hooper, J. Schnack, S. Piligkos, M. Evangelisti and E. K. Brechin, *Angew. Chem. Int. Ed.*, 2012, **51**, 4633; (g) J.-P. Peng, Q.-C. Zhang, X.-J. Kong, Y.-Z. Zheng, Y.-P. Ren, L.-S. Long, R.-B. Huang, L.-S. Zheng and Z. Zheng, *J. Am. Chem. Soc.*, 2012, **134**, 3314; (h) J.-B. Peng, Q.-C. Zhang, X.-J. Kong, Y.-P. Ren, L.-S. Long, R.-B. Huang, L.-S. Zheng and Z. Zheng, *Angew. Chem. Int. Ed.*, 2011, **50**, 10649; (i) Y. Zheng, Q.-C. Zhang, L.-S. Long, R.-B. Huang, A.Müller, J. Schnack, L.-S. Zheng and Z. Zheng, *Chem. Commun.*, 2013, **49**, 36; (j) K. C. Mondal, A. Sund, Y. Lan, G. E. Kostakis, O. Waldmann, L. Ungur, L. F. Chibotaru, C. E. Anson and A. K. Powell, *Angew. Chem. Int. Ed.*, 2012, **51**, 7550; (k) J.-P. Costes, L. Vendiera, and W. Wernsdorfer, *Dalton Trans.*, 2011, **40**, 1700; (l) K. C. Mondal, G. E. Kostakis, Y. Lan, W. Wernsdorfer, C. E. Anson and A. K. Powell, *Inorg. Chem.*, 2011, **50**, 11604; (m) E. M. Pineda, F. Tuna, Y.-Z. Zheng, S. J. Teat, R. E. P. Winpenny, J. Schnack and E. J. L. McInnes, *Inorg. Chem.*, 2014, **53**, 3032.
6. (a) V. Chandrasekhar and S. Kingsley, *Angew. Chem. Int. Ed.*, 2000, **39**, 6175; (b) V. Chandrasekhar, L. Nagarajan, K. Gopal, V. Baskar and P. Kögerler, *Dalton Trans.*, 2005, 3143; (c) V. Chandrasekhar, L. Nagarajan, R. Clérac, S. Ghosh, T. Senapati and S. Verma, *Inorg. Chem.*, 2008, **47**, 5347; (d) V. Chandrasekhar, T. Senapati and E. C. Sañudo, *Inorg. Chem.*, 2008, **47**, 9553; (e) V. Chandrasekhar and L. Nagarajan, *Dalton. Trans.*, 2009, 6712; (f) V. Chandrasekhar, D. Sahoo, R. S. Narayanan, R. J. Butcher, F. Lloret and E. Pardo, *Dalton Trans.*, 2013, **42**, 8192; (g) V. Baskar, M. Shanmugam, E. C. Sañudo, M. Shanmugam, D. Collison, E. J. L. McInnes, Q. Wei and R. E. P. Winpenny, *Chem. Commun.* 2007, 37; (h) J. A. Sheikh, H. S. Jena, A. Adhikary, S. Khatua and S. Konar, *Inorg. Chem.*, 2013, **52**, 9717.
7. (a) E. I. Tolis, M. Helliwell, S. Langley, J. Raftery and R. E. P. Winpenny, *Angew. Chem.*, 2003, **42**, 3804; (b) S. Konar and A. Clearfield, *Inorg. Chem.*, 2008, **47**, 3492; (c) S. Khanra, M. Helliwell, F. Tuna, E. J. L. McInnes and R. E. P. Winpenny, *Dalton Trans.*, 2009, 6166; (d) S. Khanra, M. Helliwell, F. Tuna, E. J. L. McInnes and R. E. P. Winpenny, *Dalton Trans.*, 2009, 6166;.
8. (a) S. Maheswaran, G. Chastanet, S. J. Teat, T. Mallah, R. Sessoli, W. Wernsdorfer and R. E. P. Winpenny, *Angew. Chem., Int. Ed.*, 2005, **44**, 5044; (b) M. Shanmugam, G. Chastanet, T. Mallah, R. Sessoli, S. J. Teat, G. A. Timco and R. E. P. Winpenny, *Chem. Eur. J.* 2006, **12**, 8777; (c) M. Shanmugam, M. Shanmugam, G. Chastanet, R. Sessoli, T. Mallah, W. Wernsdorfer and R. E. P. Winpenny, *J. Mat. Chem.* 2006, **16**, 2576.
9. (a) B. A. Breeze, M. Shanmugam, F. Tuna and R. E. P. Winpenny, *Chem. Commun.*, 2007, **47**, 5185; (b) S. K. Langley, M. Helliwell, S. J. Teat and R. E. P. Winpenny, *Inorg. Chem.*, 2014, **53**, 1128; (c) J. A. Sheikh, A. Adhikary, H. S. Jena, S. Biswas and S. Konar, *Inorg. Chem.*, 2014, **53**, 1606.
10. (a) S. Langley, M. Helliwell, R. Sessoli, S. J. Teat and R. E. P. Winpenny, *Inorg. Chem.* 2008, **47**, 497; (b) S. Langley, M. Helliwell, R. Sessoli, S. J. Teat and R. E. P. Winpenny, *Dalton Trans.*, 2009, 3102; (c) S. K. Langley, M. Helliwell, S. J. Teat and R. E. P. Winpenny, *Dalton Trans.*, 2012, **41**, 12807; (d) E. M. Pineda, F. Tuna, Y.-Z. Zheng, R. G. Pritchard, A. C. Regan, R. E. P. Winpenny, E. J. L. McInnes, *Chem. Commun.* 2013, **49**, 3522; (e) J. A. Sheikh, S. Goswami, A. Adhikary and S. Konar, *Inorg. Chem.*, 2013, **52**, 6765.
11. (a) S. Khanra, M. Kloth, H. Mansaray, C. A. Muryn, F. Tuna, E. C. Sañudo, M. Helliwell, E. J. L. McInnes and R. E. P. Winpenny, *Angew. Chem., Int. Ed.*, 2007, **46**, 5568 (b) S. Khanra, L. Batchelor, M. Helliwell, F. Tuna, E. J. L. McInnes and R. E. P. Winpenny, *J. Mol. Struct.*, 2008, **890**, 157; (c) S. Khanra, R. Shaw, M. Helliwell, F. Tuna, C. A. Muryn, E. J. L. McInnes and R. E. P. Winpenny, *Materials*, 2010, **3**, 232.
12. (a) K. H. Zangana, E. M. Pineda, J. Schnack and R. E. P. Winpenny, *Dalton Trans.*, 2013, **42**, 14045; (b) K. H. Zangana, E. M. Pineda, E. J. L. McInnes, J. Schnack and R. E. P. Winpenny, *Chem. Commun.*, 2014, **50**, 1438.
13. (a) Y. Simonov, P. Bourosh, G. Timco, S. Grebenko, M. Mazus, C. Indrichan, N. Gerbeleu, *Chem. Bull.*, 1998, **43**, 128; (b) K.

- Abdulwahab, M. A. Malik, P. O'Brien, K. Govender, C. A. Muryn, G. A. Timco, F. Tuna, R. E. P. Winpenny, *Dalton Trans.*, 2013, **42**, 196.
14. (a) G. M. Sheldrick, *Acta Crystallogr.*, 2008, **A64**, 112; (b) O. V. Dolomanov, L. J. Bourthis, R. L. Gildea, J. A. K. Howard, H. Puschmann, *J. Appl. Cryst.*, 2009, **42**, 339.
15. N. F. Chilton, R. P. Anderson, L. D. Turner, A. Soncini, K. S. Murray, *J. Comput. Chem.*, 2013, **34**, 1164.
16. S. Stoll and A. Schweiger, *J. Magn. Reson.*, 2006, **178**, 42.
17. For example, G. Christou, *Acc. Chem. Res.*, 1989, **22**, 328
18. (a) D. M. Low, G. Rajaraman, M. Helliwell, G. Timco, J. van Slageren, R. Sessoli, S. T. Ochsenbein, R. Bircher, C. Dobe, O. Waldmann, H. U. Güdel, M. A. Adams, E. Ruiz, S. Alvarez and E. J. L. McInnes, *Chem. Eur. J.* 2006, **12**, 1385; (b) R. A. Coxall, A. Parkin, S. Parsons, A. A. Smith, G. A. Timco and R. E. P. Winpenny, *J. Sol. State Chem.*, 2001, **159**, 321; (c) S. Parsons, A. A. Smith and R. E. P. Winpenny, *Chem. Commun.* 2000, 579; (d) I. M. Atkinson, C. Benelli, M. Murrie, S. Parsons and R. E. P. Winpenny, *Chem. Commun.*, 1999, 285; (e) Y.-Z. Zheng, B. A. Breeze, G. A. Timco, F. Tuna and R. E. P. Winpenny, *Dalton Trans.*, 2010, **39**, 6175.
19. Harris notation describes the binding mode as [X.Y1Y2...Yn] where X is the overall number of metal bond by the whole ligand, and each value of Y refers to the number of metal atoms attached to the different donor atoms. See supporting information and R. A. Coxall, S. G. Harris, D. K. Henderson, S. Parsons, P. A. Tasker and R. E. P. Winpenny, *Dalton Trans.*, 2000, **14**, 2349.
20. (a) E. J. L. McInnes. *Struct. Bond.*, 2006, **122**, 69; (b) J. van Slageren. *Top. Curr. Chem.*, 2012, **321**, 199.
21. A. Bencini and D. Gatteschi, "*EPR of Exchange Coupled Systems*", Springer-Verlag, Berlin 1989, reprinted Dover Publications Inc., 2012.

Linking Cr_3 triangles through phosphonates and lanthanides: synthetic, structural, magnetic and EPR studies

Karzan H. Zangana, Eufemio Moreno Pineda, Eric J. L. McInnes and Richard E. P. Winpenny



Reaction of oxo-centred chromium(III) carboxylate triangles with a lanthanide salt and *t*-butylphosphonate leads to $\{\text{Cr}_6\text{Ln}_2\}$ compounds. Magnetic and EPR studies show that the ground state of the individual chromium triangles is $S = 3/2$ and there is little communication between them.